Per2 Mutation Recapitulates the Vascular Phenotype of Diabetes in the Retina and Bone Marrow

Ashay D. Bhatwadekar,[1] Yuanqing Yan,[1] Xiaoping Qi,[2] Jeffrey S. Thinschmidt,[1] Matthew B. Neu,[1] Sergio Li Calzi,[1] Lynn C. Shaw,[1] James M. Dominiguez,[1] Julia V. Busik,[3] Choogon Lee,[4] Michael E. Boulton,[2] and Maria B. Grant[1]

In this study, we assessed whether *Per2* clock gene–mutant mice exhibit a vascular phenotype similar to diabetes. *Per2* (B6.129-Per2^{tm1Drw}/J) or wild-type control mice 4 and 12 months of age were used. To evaluate diabetes-like phenotype in *Per2* mutant mice, retina was quantified for mRNA expression, and degree of diabetic retinopathy was evaluated. Bone marrow neuropathy was studied by staining femurs for tyrosine hydroxylase (TH) and neurofilament 200 (NF-200). The rate of proliferation and quantification of bone marrow progenitor cells (BMPCs) was performed, and a threefold decrease in proliferation and 50% reduction in nitric oxide levels were observed in *Per2* mutant mice. TH-positive nerve processes and NF-200 staining were reduced in *Per2* mutant mice. Both retinal protein and mRNA expression of endothelial nitric oxide synthase were decreased by twofold. Other endothelial function genes (*VEGFR2*, *VEGFR1*) were downregulated (1.5–2-fold) in *Per2* mutant retinas, whereas there was an upregulation of profibrotic pathway mediated by transforming growth factor-β1. Our studies suggest that *Per2* mutant mice recapitulate key aspects of diabetes without the metabolic abnormalities, including retinal vascular damage, neuronal loss in the bone marrow, and diminished BMPC function. ***Diabetes*** **62:273–282, 2013**

The endogenous circadian system drives the daily timing of many physiological and behavioral processes. The circadian oscillations not only are consequences of light perception, but also are generated by endogenous circadian clocks that can adapt the physiology of an organism to its needs in an anticipatory manner. Acute pathologic events exhibit diurnal patterns; the incidence of acute myocardial infarction, myocardial ischemia, cardiac arrest, ventricular tachycardia, and sudden death caused by heart failure all vary according to the time of day (1). Circadian clocks form a series of intrinsic self-sustained transcriptional and translational feedback loops that persist in tissue even when isolated in vitro or cultured (2), and about 5–10% of transcriptome is under circadian control in the liver, heart, suprachiasmatic nucleus, aorta (3), and vertebrate retina. The predominant expression of clock genes in mammalian retina are observed in dopaminergic cells of the inner nuclear layer and in cells of the ganglion cell layer (4).

Bone marrow progenitor cells (BMPCs) show a typical diurnal pattern of release, with levels peaking during rest, while at nadir in the active phase both in humans (5) and in rodents (6), which is altered in diabetes (7–9). Reduced neuronal input to the bone marrow is deemed responsible for the dysfunctional release of these cells. Because this bone marrow neuropathy results in a reduced release of reparative progenitor cells in the circulation, we postulate that this defect in BMPC release contributes to the development of the vasodegenerative phase of diabetic retinopathy. Diabetes not only induces a circadian defect in BMPC release, but also severely compromises the reparative potential of BMPCs through proliferative, migratory defects (10) and by creating a hostile environment that prevents proper repair as a result of advanced glycation modification of the basement membrane (11). Reduced bioavailability of nitric oxide (NO) is one of the pathogenic features of dysfunction in diabetic BMPCs (12).

Per genes are at the core of the circadian clock mechanism, and phosphorylation kinetics of PER proteins dictate period length of the circadian clock. PER2 proteins undergo posttranscriptional modification, and mutations in *Per2* can abolish normal phosphorylation, leading to familial advanced sleep phase syndrome (13). *Per2* is spontaneously expressed in the retina immediately after birth, mainly in the inner part of the neuroblastic retina, and from postnatal day 1, *Per2* gradually develops into the inner nuclear layer of mature eye. Homozygous mutant mice for *Per2* show aberrant gene products for *Per2* and do not produce any functional PER2 proteins. Several transcript forms of the *mPer2* allele could, if translated, generate a truncated form of PER2 proteins lacking 108 amino acids and devoid of any activity. Mutations in *Per2* have been documented in cancer (14), increased alcohol consumption (15), altered mood behavior (16), shortened life span, and endothelial dysfunction (17).

Endothelial dysfunction is central to the underlying pathology of diabetic vascular diseases along with inadequate contribution by BMPCs to repair injured endothelium. Several studies reported the importance of *Per2* in normal endothelial function (17,18), but how *Per2* mutation influences retinal vascular function, bone marrow innervation, and the reparative ability of BMPCs have not been explored.

RESEARCH DESIGN AND METHODS

All animal studies were approved by the institutional animal care and use committee and conducted in accordance with National Institutes of Health guiding principles in the care and use of animals and the Association for Research in Vision and Ophthalmology *ARVO Statement for the Use of Animals in Ophthalmic and Vision Research*. Wild-type or *Per2* mutant (B6.129-Per2^{tm1Drw}/J) mice 4–12 months of age were maintained in a colony at animal

From the [1]Department of Pharmacology and Therapeutics, University of Florida, Gainesville, Florida; the [2]Department of Anatomy and Cell Biology, University of Florida, Gainesville, Florida; the [3]Department of Physiology, Michigan State University, East Lansing, Michigan; and the [4]Biomedical Sciences Department, Florida State University, Tallahassee, Florida.
Corresponding author: Maria B. Grant, grantma@.ufl.edu.
Received 17 February 2012 and accepted 16 July 2012.
DOI: 10.2337/db12-0172
This article contains Supplementary Data online at http://diabetes.diabetesjournals.org/lookup/suppl/doi:10.2337/db12-0172/-/DC1.

See accompanying commentary, p. 29.

care facilities of Florida State University. At study termination, the animals were killed by an overdose of ketamine 14 mg/kg and xylazine 30 mg/kg.

Trypsin digestion of mouse retina. Trypsin digestion of retina was performed as described previously (19), and the number of acellular capillaries per square millimeter of retina were quantified.

Endothelial nitric oxide synthase staining of mouse retina. Retinal trypsin digests were stained with anti-endothelial nitric oxide synthase (eNOS) antibodies (Sigma-Aldrich, St. Louis, MO) followed by staining with fluorescein isothiocyanate (FITC)-conjugated secondary antibodies (Invitrogen, Carlsbad, CA).

Retinal permeability and tight junction staining. Retinal permeability was assessed after tail vein injections of FITC-albumin 20 mg/kg (Sigma-Aldrich), as explained previously (20). In parallel experiments, flat-mounted retinas were stained for claudin-5 (Abcam, Cambridge, MA) and vascular endothelial (VE)-cadherin (Cell Signaling Technology, Inc., Danvers, MA). Digital images of flat-mounted retinas were obtained using a confocal microscope (Olympus DSU-Olympus IX81, Olympus America, Inc., Center Valley, PA).

Quantitative RT-PCR for mRNA expression. Equal amounts of total retinal RNA were reverse transcribed using iScript (Bio-Rad, Hercules, CA). Gene-specific primers for eNOS, inducible nitric oxide synthase (iNOS), vascular endothelial growth factor (VEGF) and receptors VEGFR1 and VEGFR2, transforming growth factor-β1 (TGF-β1), connective tissue growth factor (CTGF), plasminogen activator inhibitor 1 (PAI-1), and ID-1 (Applied Biosystems, Foster City, CA) were used to run quantitative RT-PCR. All genes were normalized to mouse TATA-binding protein.

Quantification of BMPCs. BMPCs were quantified as lin^- $sca1^+$ $c\text{-}Kit^+$ (LSK) cells using flow cytometry. Lin cells were stained with biotin mouse lineage panel followed by FITC-streptavidin (eBioscience, San Diego, CA), whereas sca1 and c-kit cells were stained using PE-rat anti-mouse Ly-6A/E and APC rat anti-mouse CD117 (BD Pharmingen), respectively.

Quantification of NO by DAF-FM fluorescence. NO was quantified from LSK cells as described previously (21).

Colony-forming assay for mouse hematopoietic stem cells. Bone marrow mononuclear cells (1×10^4) were plated for assay using MethoCult (STEMCELL Technologies Inc.), and numbers of colonies were enumerated at 7–10 days.

Tyrosine hydroxylase and neurofilament 200 staining of bone marrow. Tyrosine hydroxylase (TH) and neurofilament 200 (NF-200) staining of femurs was performed as described previously (7).

Assessment of vascularity in sciatic nerves. Sciatic nerve vascularity was assessed by in situ staining with rhodamine-conjugated *Bandeiraea simplicifolia* (BS)-1 isolectin (Vector Laboratories), and the number of vessels were quantified by transverse sectioning.

Statistical analyses. All results are expressed as mean ± SEM. The comparisons for more than two groups were analyzed using one-way ANOVA

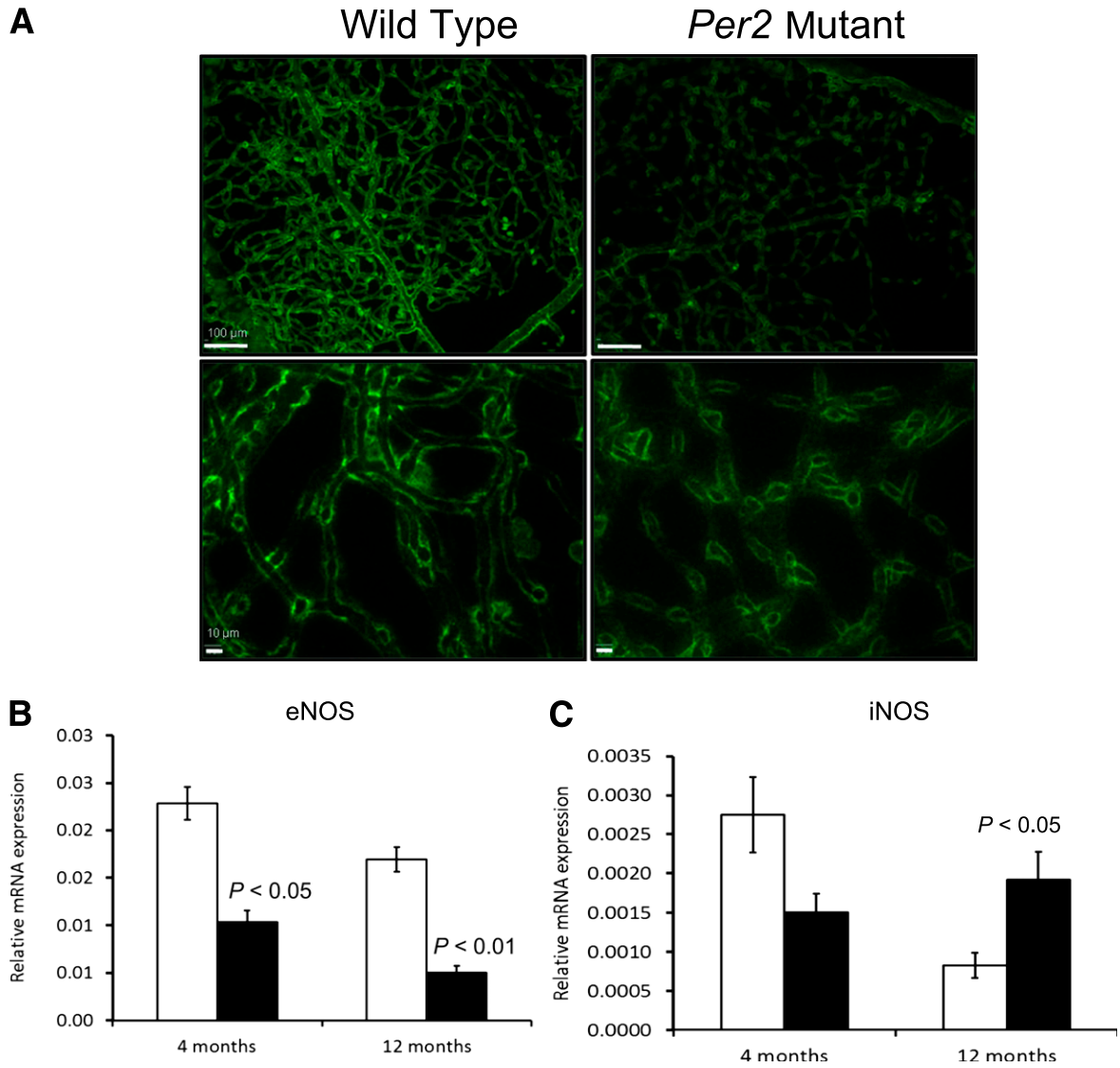

FIG. 1. *Per2* mutant retinas showed reduced eNOS but increased iNOS expression. Wild-type and *Per2* mutant retinas were trypsin digested and stained for eNOS expression (*A*). Flat-mounted retinas showed reduced expression of eNOS in *Per2* mutant mice compared with wild-type controls at 12 months of age. The images from both wild-type and *Per2* mutant mice were taken while keeping constant settings (exposure, brightness, and contrast) for the microscope. Retinas from both 4- and 12-month-old wild-type and *Per2* mutant mice were evaluated for eNOS (*B*) and iNOS (*C*) mRNA expression using quantitative RT-PCR. *n* = 7 for 4-month-old mice; *n* = 3 for 12-month-old mice. Scale bars, 100 μm (*top panel*); 10 μm (*bottom panel*).

followed by Student-Newman-Keuls post hoc analysis. Unpaired two-tailed Student *t* test was used for two-group comparisons, whereas data for glucose tolerance tests were analyzed using two-way ANOVA followed by Bonferroni test. All the statistical tests were performed using GraphPad (La Jolla, CA) software. $P < 0.05$ was considered statistically significant.

RESULTS

***Per2* mutant mice are normoglycemic.** To determine whether *Per2* mutation alters mouse metabolism, we measured HbA_{1c} and blood glucose levels and body weight of wild-type and *Per2* mutant mice. There was no significant difference in blood glucose levels at either age; however, in 12-month-old mice, there was an insignificant increase (wild type 4.1 ± 0.081%, *Per2* mutant 4.6 ± 0.088%) in HbA_{1c} levels in the *Per2* mutant mice (Supplementary Table 1).

To assess the possibility of glucose intolerance in the *Per2* mutant mice, we performed glucose tolerance tests on 12-month-old mice. After injection of glucose 2 g/kg, plasma glucose levels showed a sharp increase in both wild-type and *Per2* mutant mice. Both groups showed recovery in blood glucose 1 h postinjection; however, *Per2* mutant mice showed a significant decrease in blood glucose level ($P < 0.01$). Moreover, the recovery after glucose challenge was better in *Per2* mutant mice at 2 h (Supplementary Fig. 1).

Decrease in eNOS expression in the retina of *Per2* mutant mice. Retinal digests prepared from *Per2* mutant animals showed less eNOS immunoreactivity (Fig. 1*A*). To study whether the decrease in protein expression of eNOS correlated with gene expression, eNOS mRNA expression was studied. A twofold decrease ($P < 0.05$) in eNOS mRNA was observed in *Per2* mutant animals at both ages (Fig. 1*B*). At 12 months, the eNOS decrease was accompanied by a dramatic increase in iNOS expression ($P < 0.05$) in *Per2* mutant mice, whereas wild-type mice showed a decrease in iNOS mRNA expression at 12 versus 4 months of age (Fig. 1*C*).

***Per2* mutant mice show an increase in acellular capillaries.** Trypsin digestion of retinas was performed to assess whether *Per2* mutation results in retinal endothelial damage. Quantification of acellular capillaries in the retina provides a direct measure of degree of retinal vascular injury. *Per2* mutant mice showed a 40% increase ($P < 0.05$) in the number of acellular capillaries, suggesting an accelerated progression of vascular dysfunction in *Per2* mutant retinas (Fig. 2*A* and *B*).

Increase in retinal permeability in *Per2* mutant mice. To determine whether an increase in acellular capillary numbers in *Per2* mutant mice is also accompanied by alteration in vascular permeability, in vivo permeability assay was performed. As shown in Fig. 3*A*, we observed a profound increase in retinal vascular leakage of FITC-albumin in *Per2* mutant retinas compared with negligible leakage of albumin in wild-type retinas.

To evaluate blood-retinal barrier integrity, immunohistochemical analysis in parallel experiments of retinal flat mounts for claudin-5 and VE-cadherin was performed. Wild-type retinas showed clearly demarcated lateral membranes of endothelial cells, exhibiting integrity of junctional

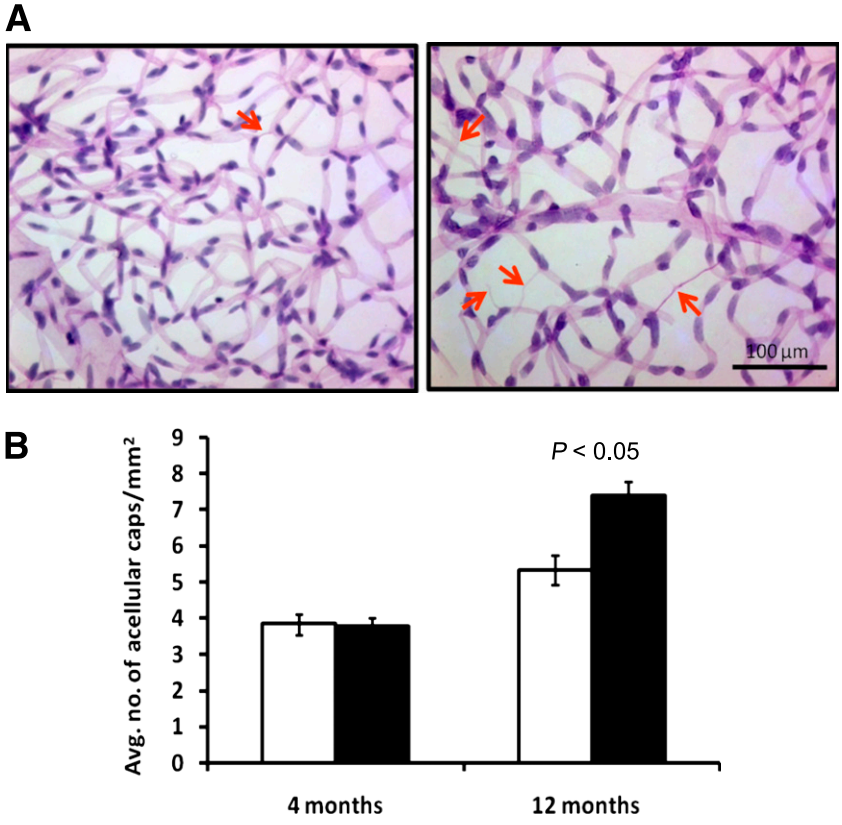

FIG. 2. *Per2* mutant retinas showed increases in acellular capillaries. Whole eyes from wild-type or *Per2* mutant mice underwent trypsin digestion followed by staining with periodic acid Schiff and counterstaining with hematoxylin. *A*: Representative images from retinas of wild-type and *Per2* mutant mice showed acellular capillaries (arrows). *B*: Quantification of retinas showed a significant increase in number of acellular capillaries in 12-month-old *Per2* mutant animals. $n = 5$ for 4-month-old mice; $n = 3$ for 12-month-old mice; white bars, wild type; black bars, *Per2* mutant.

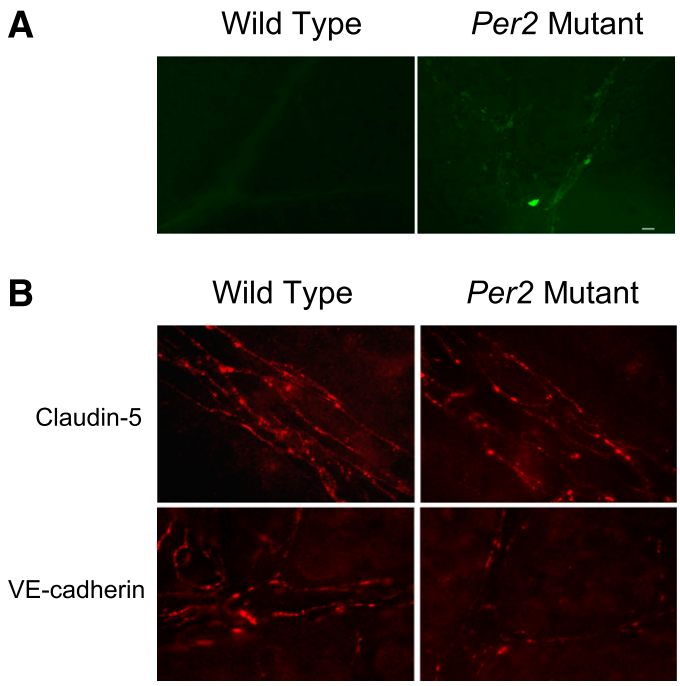

FIG. 3. Increase in retinal permeability and redistribution of claudin-5 and VE-cadherin junctional complexes in *Per2* mutant mice. *A*: Wild-type or *Per2* mutant mice injected with FITC-albumin 20 mg/kg i.v. were killed 2 h later by cardiac perfusion using 4% paraformaldehyde. Flat-mounted retinas were imaged using a confocal scanning microscope. Representative retinal flat mounts showed leakage of FITC-albumin in the retina of *Per2* mutant mice, whereas wild-type mice retinas showed background autofluorescence without any obvious albumin leakage. *B*: The neural retinas were stained for detection of claudin-5 and VE-cadherin followed by secondary staining with Cy3-conjugated goat anti-rabbit IgG antibodies. Digital confocal images were captured with identical photomultiplier tube gain settings using imaging software. Maximum projections generated from z-section stacks of confocal images were processed identically for experimental and control retinas. Images depict changes in claudin-5 and VE-cadherin localization in the retinas of *Per2* mutant mice, whereas wild-type mice showed a normal expression pattern for these proteins. $n = 5$ for wild type; $n = 5$ for *Per2* mutant Scale bar, 10 μm.

complexes for both claudin-5 and VE-cadherin. In contrast, *Per2* mutant retinas showed significant attenuation of claudin-5 expression and dissociation of cadherin junctions (Fig. 3*B*).

Increased expression of TGF-β1 and downstream mediators of TGF-β1 action in *Per2* mutant retina. To further explore the mechanism of the vascular dysfunction observed, we examined established markers of retinal vascular pathology. As shown in Fig. 4*A* and *B*, we observed a 1.5- and 2-fold decrease in VEGFR2 and VEGFR1 expression, respectively, in *Per2* mutant retinas at 12 months of age ($P < 0.001$). However, there was no change in VEGF expression in either age group (Fig. 4*C*), and *Per2* mutant retinas formed similar numbers of branch points and possessed equivalent vessel length (data not shown) compared with wild-type mouse retinas.

TGF-β1 and its downstream effectors, including CTGF, PAI-1, ID-1, and fibronectin (FN), have been implicated in both microvascular and macrovascular disease. *Per2* mutant mice showed an increase in TGF-β1 mRNA levels in retina at both 4 and 12 months of age, but this was not statistically significant (Fig. 4*D*). PAI-1, the major target gene of TGF-β1, was increased twofold ($P < 0.05$) at 4 months of age in the *Per2* mutant mice (Fig. 4*E*). ID-1, a critical mediator of TGF-β1 and cell differentiation, was increased twofold ($P < 0.05$) in 12-month-old *Per2* mutant mice (Fig. 4*F*). CTGF, an important downstream mediator of profibrotic effects of TGF-β1, has been implicated in vascular dysfunction (22). A 2.5–3-fold increase in CTGF expression was observed in *Per2* mutant retinas ($P < 0.05$) (Fig. 4*G*). At 4 months of age, retinas of *Per2* mutant mice showed a 2.5-fold increase ($P < 0.05$) (Fig. 4*H*) in FN expression, suggesting a potential role of extracellular matrix proteins in the progression of retinal vascular dysfunction; however, no difference was observed at 12 months of age.

Dysfunction in BMPC release from bone marrow in *Per2* mutant mice. To study the contribution of BMPCs in developing retinal vascular dysfunction, the numbers of LSK cells were quantified in bone marrow using flow cytometry. The bone marrow was flushed; erythrocytes were lysed; and after washing with PBS, the mononuclear cells were incubated with sca1 and c-kit antibodies. Figure 5*A* shows the hierarchy of flow cytometry gating. The LSK cell population was gated based on low side scatter (gate 1); typically, blood cells smaller in size with a single nucleus (e.g., monocytes, lymphocytes) and BMPCs can be efficiently gated using this strategy. By using successive gating, positively stained $sca1^+$ cells were subsequently gated for the lin^- and $sca1^+$ populations (gate 2). This population was further separated for $sca1^+$ and $c\text{-}kit^+$ populations to determine the LSK^+ population. Quantification of the LSK population showed that 4-month-old *Per2* mutant mice showed twofold more cells (Fig. 5*B*) ($P < 0.05$) within the bone marrow, suggesting an inability of *Per2* mutant BMPCs to egress from the bone marrow. There was a dramatic decrease (~200 times) in number of BMPCs in both wild-type and *Per2* mutant mice at 12 months of age, which may be attributed to aging and progressive bone marrow exhaustion (Fig. 5*B*).

BMPCs of *Per2* mutant mice show decreased colony formation and NO levels. Methylcellulose colony-forming assays provide a direct estimate of BMPC proliferative potential. To determine whether bone marrow cells from *Per2* mutant mice possess impaired proliferation, mononuclear cells were propagated on methylcellulose cultures, and the number of colonies was quantified at 7 days. Wild-type animals exhibited robust colony formation (Fig. 6*A*), whereas a dramatic decrease in number of colonies of *Per2* mutant animals was observed. Quantification of number of colonies showed a threefold decrease ($P < 0.05$) in *Per2* mutant mice at both ages (Fig. 6*B*). To further characterize dysfunction in BMPCs, NO concentration in BMPCs was quantified using DAF-FM fluorescence. BMPCs obtained from *Per2* mutant mice showed a 1.5-fold decrease in NO levels ($P < 0.05$) (Fig. 6*C*).

Bone marrow neuropathy in *Per2* mutant mice. TH is a rate-limiting step in catecholamine synthesis, which directly contributes to the release of BMPCs. To determine the number of TH-positive nerve fibers, femurs were sectioned, and immunohistochemical staining for TH was performed. Bone marrow of both wild-type and *Per2* mutant mice showed positive staining of TH nerve fibers adjacent to blood vessels (Fig. 7*A*); however, 4-month-old *Per2* mutant mice showed a dramatic increase in TH-positive nerve processes ($P < 0.05$) compared with wild-type controls. In contrast, by 12 months of age, a fivefold decrease ($P < 0.05$) in TH staining in the *Per2* mutant animals was observed compared with wild-type controls (Fig. 7*B*). These fluctuations in TH staining suggest modulation of noradrenergic neurons. To assess whether these changes were associated with a change in total innervations, NF-200 staining was performed. Figure 7*C* shows fewer NF-200-positive nerve processes in *Per2* mutant

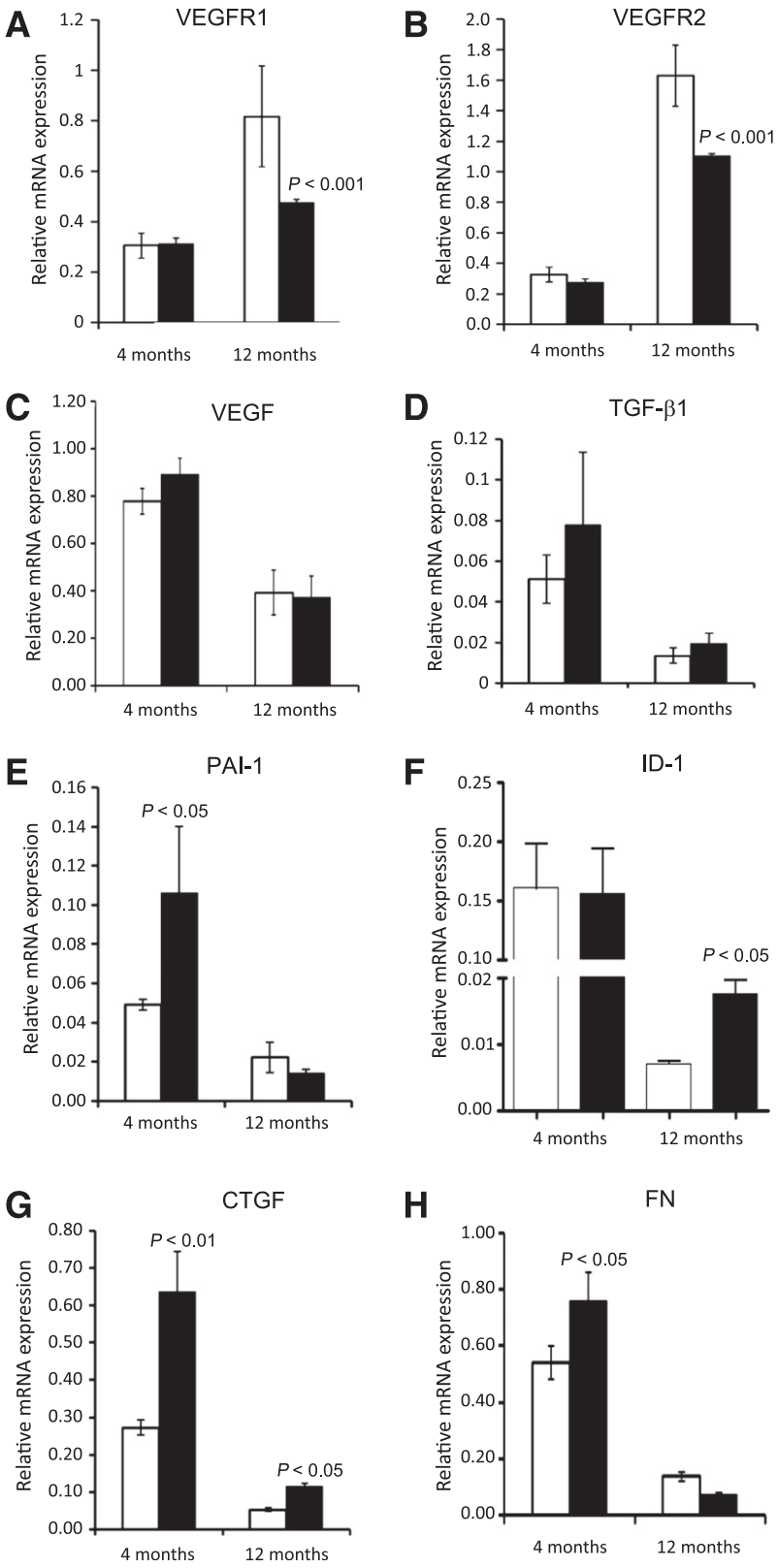

FIG. 4. Decrease in VEGF receptor expression and upregulation of TGF-β-induced profibrotic gene expression in *Per2* mutant retinas. There was no significant change in VEGFR1 (*A*) or VEGFR2 (*B*) expression in retinas of 4-month-old *Per2* mutant mice; however, there was a dramatic decrease in mRNA expression of both receptor expressions in 12-month-old animals. VEGF expression remained unchanged in both groups (*C*). *Per2* mutant retinas showed a profound increase in mRNA expression of TGF-β1 (*D*) and its downstream effectors PAI-1 (*E*), ID-1 (*F*), CTGF (*G*), and FN (*H*). The most prevalent change in mRNA expression was observed in 4-month-old *Per2* mutant mice for TGF-β1, PAI-1, and FN, whereas ID-1 expression was significantly increased in 12-month-old *Per2* mutant mice. CTGF mRNA was increased in both age groups. *n* = 7 for 4-month-old mice; *n* = 3 for 12-month-old mice; white bars, wild type; black bars, *Per2* mutant.

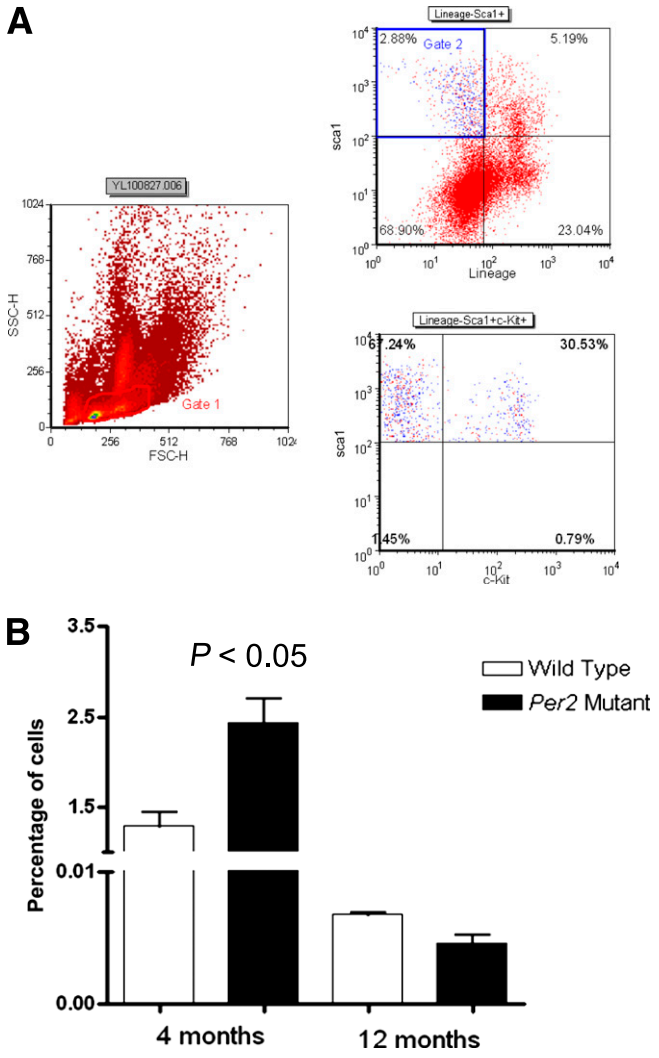

FIG. 5. Dysfunctional release of BMPCs in *Per2* mutant mice. Femoral bone marrow was stained for LSK antibodies, and the percentage of cells was quantified using flow cytometry. *A*: Typical flow cytometry dot plot showing selective gating strategy for characterizing LSK cells. *B*: Quantification of LSK cells showed an increase in the number of cells trapped in the bone marrow of 4-month-old *Per2* mutant animals, suggesting difficulty in their release. The numbers of LSK cells were significantly decreased in 12-month-old mice in both groups, and the difference in respective groups was negligible. $n = 7$ for 4-month-old mice; $n = 3$ for 12-month-old mice. FSC-H, forward scatter height; SSC-H, side scatter height.

animals. Quantification of NF-200 nerve processes showed a 20 and 30% decrease ($P < 0.05$) in 4- and 12-month-old *Per2* mutant animals, respectively, compared with age-matched wild-type controls (Fig. 7*D*). To determine whether neural vascularity was mediating the bone marrow changes, we studied the vasa nervorum of sciatic nerves using an injection of rhodamine-conjugated BS-1 lectin before the animals were killed. *Per2* mutant mice showed a reduction in the number of vessels (Fig. 8*A*). Quantification of neural vascularity showed an ~25% decrease ($P < 0.05$) in number of vessels in *Per2* mutant mice (Fig. 8*B*).

DISCUSSION

Alterations in circadian rhythm are associated with several pathological conditions, including sleep disorders, cardiovascular diseases, and metabolic syndrome. The *Per2* clock gene plays a central role in resetting the clock, and mutations in *Per2* have been associated with endothelial dysfunction, limb ischemia, and early vascular senescence. Diabetic animals show altered circadian rhythm, with phase advancement resulting in contractile dysfunction (23). *Clock* and *Bmal-1* pancreatic conditional knockout mice show hypoinsulinemia and develop type 1 diabetes (24). Previously, we reported that diabetes results in circadian dysregulation of BMPC release and a decrease in mRNA expression for *Per2* in these cells and in retina (7).

In the present study, we show that *Per2* mutant mice exhibit progressive retinal vascular dysfunction with an increase in acellular capillaries and retinal permeability, reduced eNOS expression, and upregulation of profibrotic genes. Additionally, *Per2* mutant retinas show dissociation of tight junctions and adherens junctional integrity. These retinal changes are accompanied by bone marrow neuropathy with increased numbers of BMPCs retained within the bone marrow, suggesting reduced release of these cells into the circulation similar to what we observed in both type 1 and type 2 diabetic rats. However, the *Per2* mutant animals show blood glucose and HbA_{1c} levels similar to wild-type mice. Previous studies indicated that *Per2* mutant mice exhibit low blood pressure and normal serum lipid levels. More importantly, *Per2* mutant mice possess faster glucose clearance than wild-type animals (25,26). Consistent with previous reports, the present glucose tolerance test indicates faster clearance and recovery of blood glucose in 12-month-old *Per2* mutant mice compared with wild-type controls. This finding indicates that the dysfunction associated with *Per2* mutant mice is not a result of elevated glucose levels, lipid levels, or blood pressure but, rather, is directly linked to loss of *Per2*. *Per2* is an important component of the glucocorticoid regulatory pathway, and disruption of glucocorticoid regulation and leptin regulation may be partly responsible for the enhanced glucose sensitivity observed in the *Per2* mutant mice (26).

We also observed a decrease in retinal eNOS expression in *Per2* mutant mice similar to that found in diabetes (27). Diabetes-associated deficiency in endothelium-derived NO coupled with activation of iNOS can generate large amounts of highly reactive oxygen species. Increased expression of iNOS has been reported in the retinas of both humans (28) and experimental animals (29). Furthermore, we previously showed that eNOS knockout mice made diabetic exhibit an acceleration of diabetic retinopathy (30) characterized by increased retinal vessel leakage, gliosis, numbers of acellular retinal capillaries, and basement membrane thickening of retinal capillaries. Functional loss of *Per2* impairs endothelial function in mouse aortas and results in reduced NO production, reduced expression of the vasodilatory prostaglandin PGI (2), and increased release of cyclooxygenase (COX)-1; however, COX-2 expression was undetected (17). Although both COX-1 and COX-2 have been ubiquitously identified on ocular tissues, such as amacrine cells, ganglion cells, horizontal cells, microglia, and Müller cells (31), several reports suggested that COX-2 is the predominant mediator of vascular dysfunction acting through increasing VEGF production (32,33). However, we did not see any change in expression of retinal VEGF in *Per2* mutant mice, suggesting a lack of involvement of the COX pathway in retinal vascular dysfunction.

TGF-β and its downstream effectors are implicated in the pathogenesis of diabetic retinal vascular dysfunction.

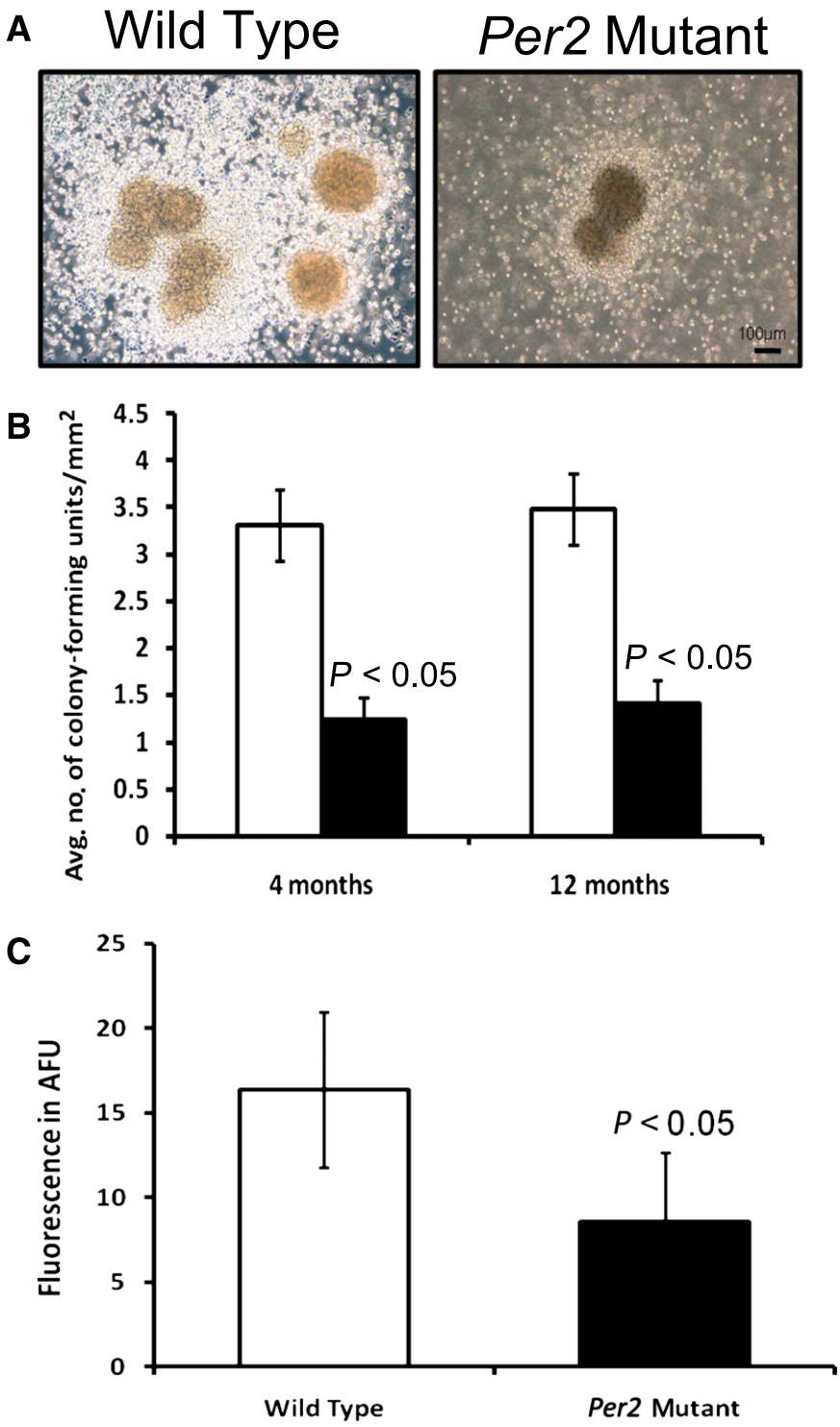

FIG. 6. Decrease in proliferation and NO of *Per2* mutant animals. *A*: 1×10^4 mouse bone marrow mononuclear cells were placed on methylcellulose semisolid media under well-humidified conditions. After 7 days, colony-forming units were detected in *Per2* mutant and wild-type mice. Representative images from colony-forming units of wild-type or *Per2* mutant mice are shown. *B*: Quantification of colony-forming units showed a significant decrease in numbers of colony-forming units in *Per2* mutant mice compared with wild-type control. *C*: BMPCs isolated from *Per2* mutant mice showed a significant decrease in expression of NO as determined by DAF-FM fluorescence. *n* = 7 for 4-month-old mice; *n* = 3 for 12-month-old mice; white bars, wild type; black bars, *Per2* mutant. AFU, arbitrary fluorescence unit. (A high-quality color representation of this figure is available in the online issue.)

In the present study, *Per2* mutant retinas exhibited a dramatic increase in expressions of PAI-1 and FN, suggesting the predominant role of extracellular matrix alterations in pathogenesis of vascular dysfunction in these animals. Expression of CTGF, an important downstream mediator of profibrotic effects of TGF-β, is increased early on in the retinas of diabetic mice (34). Retinal mRNA data obtained in the present study support this notion. Moreover, we speculate that CTGF may be one of the predominant mediators of vascular dysfunction in *Per2* mutant retinas.

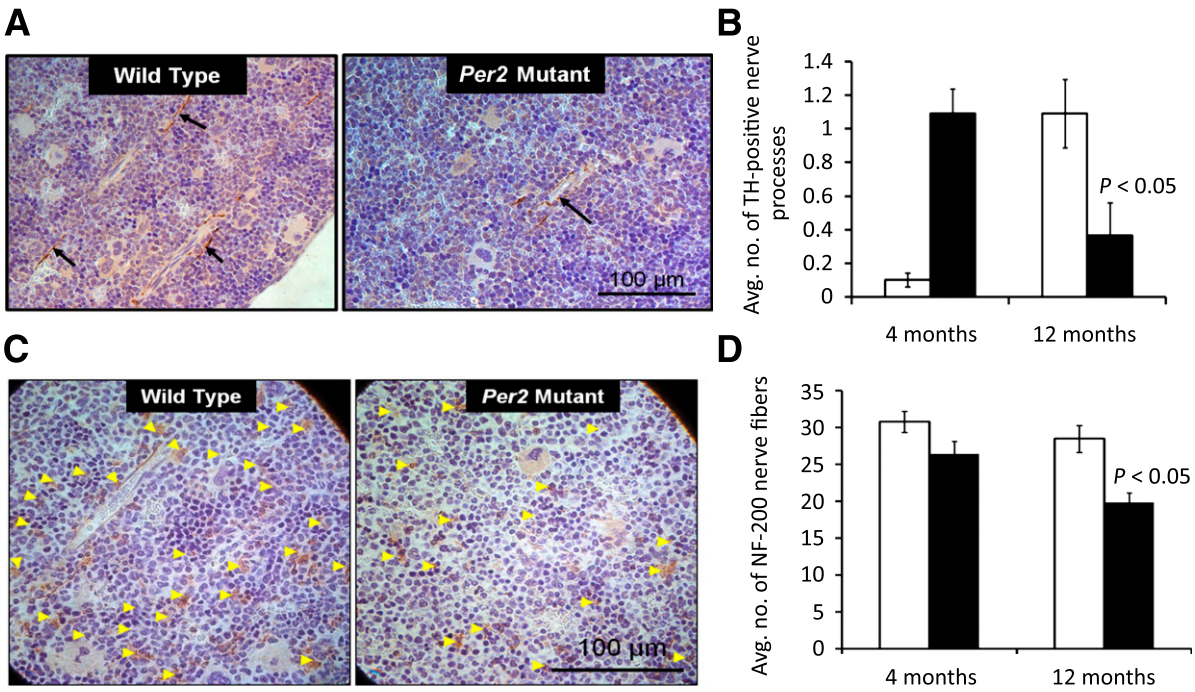

FIG. 7. Bone marrow neuropathy in *Per2* mutant mice. Femurs collected from wild-type or *Per2* mutant mice were decalcified paraffin embedded, sectioned on microtome at 4 μm, and stained for TH or NF-200. *A*: Representative images from TH-labeled bone marrow show TH expression near blood vessels (arrows). *B*: *Per2* mutant bone marrow exhibited a dramatic reduction in TH labeling in 12-month-old animals, whereas an increase in TH expression in 4-month-old mice was found. *C*: *Per2* mutant femurs were evaluated for bone marrow neural activity using NF-200 immunohistochemistry; photomicrographs show neurofilaments labeled with NF-200 (arrowheads) for 12-month-old mice. *D*: Quantification of NF-200 labeling showed a decrease in NF-200 expression in both 4- and 12-month-old mice. *n* = 7 for 4-month-old mice; *n* = 3 for 12-month-old mice; white bars, wild type; black bars, *Per2* mutant.

Loss of *Per2* results in activation of β-catenin (35), an essential effector of the Wnt signaling pathway that is also involved in increasing CTGF expression (36) in the diabetic retina (37). Although the precise source of CTGF in the retina is not clear from the present study, previous reports showed that profibrotic factors involved in basement membrane thickening of retinal capillaries in diabetes are mainly expressed in pericytes (38), suggesting that future studies need to evaluate pericytes in *Per2* mutant mice.

Of note, a significant decrease in VEGFR1 and VEGFR2 mRNA expression occurred at 12 months of age in *Per2* mutant retinas; however, the total number and branching of retinal vessels was not different in these mice compared with controls. The increase in mRNA expression of VEGFR1 and VEGFR2 may reflect an age-associated capillary enlargement (39). The mechanism responsible for VEGF and VEGF receptor modulation of angiogenesis is complex. VEGFR1 regulates angiogenesis through ligand trapping or receptor heterodimerization, whereas VEGFR2 stimulates a variety of pathways controlling endothelial growth, differentiation, migration, and tubulogenesis (40). Although VEGF expression is increased in retinas of diabetic rats (41), we did not see any change in VEGF mRNA expression at either age in the *Per2* mutant mice. Thus, taken together, the present study suggests that morphologically and metabolically, *Per2* mutant mice are similar to wild-type mice wherein the predominant mechanism in the development of acellular capillaries involves reduced eNOS expression with a concomitant increase in proinflammatory and profibrotic markers promoting extracellular matrix thickening.

The present data indicate that the inability of BMPCs to enter the circulation can contribute to vascular dysfunction in *Per2* mutant mice. Moreover, we observed a reduction in proliferative potential of BMPCs from *Per2* mutant mice. This finding agrees with a typical phenotype of type 2 diabetes in a previous report, which suggested that bone marrow neuropathy results in altered release and proliferation of BMPCs (7). Orlandi et al. (42) reported that long-term diabetes specifically reduces long-term repopulating BMPCs and their proliferative potential. We also observed a similar decrease in numbers of BMPCs and colony-forming response of BMPC obtained from type 1 diabetic mice (Hazra et al. [43]). We observed a >94% decline of BMPCs after 12 months of diabetes. Precisely how *Per2* mutation controls cell proliferation is intriguing. Downregulation of *Per2* in cancer cell lines increases β-catenin protein levels and the β-catenin target protein cyclin D, accelerating cancer cell proliferation (35). *Per2* mutation in endothelial cells is associated with upregulation of Akt signaling and phosphoinositide-dependent kinase-1 (PDK-1) (44). Activation of Akt/PDK-1 inactivates and phosphorylates forkhead box O (FOXO) proteins (45), which are critical in maintaining long-term repopulating of BMPC because of their ability to regulate oxidative stress (46). We believe that the decrease in FOXO levels after chronic activation of Akt is a possible mechanism for the decreased proliferation of BMPCs we observed. However, further studies are necessary to delineate the exact mechanism. We also observed a reduction in NO levels (the critical regulator of cell migration) in BMPCs isolated from the *Per2* mutant mice similar to that in BMPCs isolated from diabetic mice (12). Thus, we believe that the cumulative dysfunction of proliferation, migration, and release of BMPCs can severely compromise vascular repair and may be responsible for the retinal vascular pathology we observed in *Per2* mutant mice.

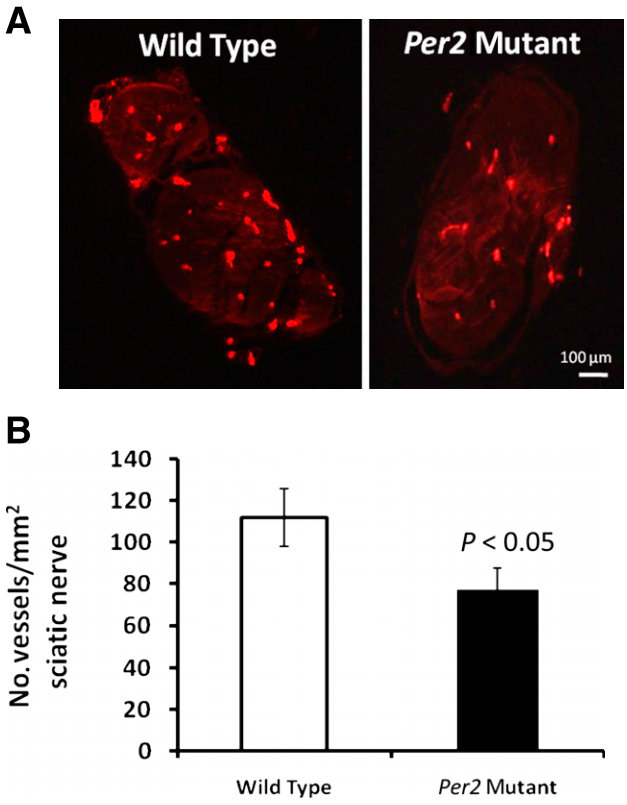

FIG. 8. Reduction in vasa nervorum in *Per2* mutant mice. Wild-type or *Per2* mutant mice were injected with rhodamine-conjugated BS-1 isolectin 0.1 mg/mouse before kill, and the sciatic nerve was harvested, paraffin embedded, and cut transversally. *A*: Representative photomicrographs show that the network of vasa nervorum was markedly reduced in *Per2* mutant mice compared with wild-type controls. Ten sections per animal were counted using ImageJ software, and the number of vessels per square millimeter of sciatic nerve was determined. *B*: A significant reduction in neural vascularity in *Per2* mutant mice was found compared with wild-type controls. n = 6 for wild type; n = 7 for *Per2* mutant.

The bone marrow microenvironment exerts a selective inhibitory role on adherent progenitors, controlling their release into the circulation while maintaining their proliferative potential in bone marrow. Bone marrow nerve fibers run along vessels within bone marrow parenchyma (47). Neurotransmitters released by the sympathetic nervous system regulate retention and release of BMPCs. However, we did not see any change in retinal expression of TH or NF-200 (Supplementary Figs. 2 and 3), which suggests that bone marrow neuropathy plays a key role in vascular dysfunction in *Per2* mutant mice. TH, the rate-limiting step in norepinephrine synthesis, is reported to be decreased in diabetes (7); similarly, we show that *Per2* mutant mice exhibit a decrease in TH nerve fibers at 12 months of age. However, much to our surprise, there was a dramatic increase in TH activity in 4-month-old animals. This may result from inhibition of monoamine oxidase, which has also been observed in *Per2* mutant mice (16), and suggests, perhaps, that we are observing a compensation in response to an overall decrease in the number of nerve fibers.

Diabetic neuropathy is caused by both imbalances in neuron metabolism and impaired nerve blood flow. Maintenance of an adequate supply of blood through the vasa nervorum is essential to prevent neuropathy (48). The sciatic nerve of diabetic mice possesses reduced motor and sensory nerve conduction velocities, blood flow, and capillary density (49). We observed a similar decrease in capillary density in sciatic nerves of *Per2* mutant mice, which may be a result of a reduction of NO levels in sciatic nerve and vasa vasorum, leading to early vascular senescence and BMPC dysfunction as reported previously (44).

While acknowledging that mutation of retinal *Per2* may also have a profound effect on retinal vascular dysfunction, the present study suggests that bone marrow neuropathy is linked to retinopathy in *Per2* mutant mice. First, the decrease in neural vascularity of *Per2* mutant mice contributes to reduced sympathetic neurotransmission. Second, the loss of neurotrophic support may lead to changes in the bone marrow microenvironment, resulting in BMPCs with reduced proliferative potential as well as reduced release into the circulation, limiting their participation in vascular repair. Finally, together with reduced eNOS and hyperactive profibrotic TGF-β1, this retinal vasculature and bone marrow pathology can lead to the development of acellular capillaries as a result of both endothelial dysfunction and reduced endothelial repair.

ACKNOWLEDGMENTS

This work was supported by an American Heart Association Post-Doctoral Award and a Thomas H. Maren Junior Investigator award to A.D.B. and National Institutes of Health Grants EY-018358 to M.E.B. and EY-007739, EY-012601, U01-HL-087366, and DK-090730 to M.B.G. M.B.N. is supported by the UF-HHMI Science for Life program.

No potential conflicts of interest relevant to this article were reported.

The funder played no role in the conduct of the study, collection of data, management of the study, analysis of data, interpretation of data, or preparation of the manuscript.

A.D.B. conducted experiments and wrote the manuscript. Y.Y., X.Q., J.S.T., M.B.N., S.L.C., L.C.S., and J.M.D. helped with experiments. J.V.B., C.L., and M.E.B. reviewed and edited the manuscript. M.B.G. wrote the manuscript and helped with discussion and editing. A.D.B. and M.B.G. are the guarantors of this work and, as such, had full access to all the data in the study and take responsibility for the integrity of the data and the accuracy of the data analysis.

The authors thank Marda Jorgensen, McKnight Brain Institute, University of Florida, Gainesville, Florida, for technical assistance.

REFERENCES

1. Muller JE, Ludmer PL, Willich SN, et al. Circadian variation in the frequency of sudden cardiac death. Circulation 1987;75:131–138
2. Reppert SM, Weaver DR. Coordination of circadian timing in mammals. Nature 2002;418:935–941
3. Rudic RD, McNamara P, Reilly D, et al. Bioinformatic analysis of circadian gene oscillation in mouse aorta. Circulation 2005;112:2716–2724
4. Witkovsky P, Veisenberger E, LeSauter J, et al. Cellular location and circadian rhythm of expression of the biological clock gene Period 1 in the mouse retina. J Neurosci 2003;23:7670–7676
5. Tsinkalovsky O, Smaaland R, Rosenlund B, et al. Circadian variations in clock gene expression of human bone marrow CD34+ cells. J Biol Rhythms 2007;22:140–150
6. Méndez-Ferrer S, Lucas D, Battista M, Frenette PS. Haematopoietic stem cell release is regulated by circadian oscillations. Nature 2008;452:442–447
7. Busik JV, Tikhonenko M, Bhatwadekar A, et al. Diabetic retinopathy is associated with bone marrow neuropathy and a depressed peripheral clock. J Exp Med 2009;206:2897–2906
8. Ando H, Takamura T, Matsuzawa-Nagata N, et al. Clock gene expression in peripheral leucocytes of patients with type 2 diabetes. Diabetologia 2009;52:329–335

9. Kreier F, Kalsbeek A, Sauerwein HP, Fliers E, Romijn JA, Buijs RM. "Diabetes of the elderly" and type 2 diabetes in younger patients: possible role of the biological clock. Exp Gerontol 2007;42:22–27
10. Caballero S, Sengupta N, Afzal A, et al. Ischemic vascular damage can be repaired by healthy, but not diabetic, endothelial progenitor cells. Diabetes 2007;56:960–967
11. Bhatwadekar AD, Glenn JV, Li G, Curtis TM, Gardiner TA, Stitt AW. Advanced glycation of fibronectin impairs vascular repair by endothelial progenitor cells: implications for vasodegeneration in diabetic retinopathy. Invest Ophthalmol Vis Sci 2008;49:1232–1241
12. Segal MS, Shah R, Afzal A, et al. Nitric oxide cytoskeletal-induced alterations reverse the endothelial progenitor cell migratory defect associated with diabetes. Diabetes 2006;55:102–109
13. Toh KL, Jones CR, He Y, et al. An hPer2 phosphorylation site mutation in familial advanced sleep phase syndrome. Science 2001;291:1040–1043
14. Fu L, Pelicano H, Liu J, Huang P, Lee C. The circadian gene Period2 plays an important role in tumor suppression and DNA damage response in vivo. Cell 2002;111:41–50
15. Spanagel R, Pendyala G, Abarca C, et al. The clock gene Per2 influences the glutamatergic system and modulates alcohol consumption. Nat Med 2005;11:35–42
16. Hampp G, Albrecht U. The circadian clock and mood-related behavior. Commun Integr Biol 2008;1:1–3
17. Viswambharan H, Carvas JM, Antic V, et al. Mutation of the circadian clock gene Per2 alters vascular endothelial function. Circulation 2007;115:2188–2195
18. Reilly DF, Westgate EJ, FitzGerald GA. Peripheral circadian clocks in the vasculature. Arterioscler Thromb Vasc Biol 2007;27:1694–1705
19. Bhatwadekar A, Glenn JV, Figarola JL, et al. A new advanced glycation inhibitor, LR-90, prevents experimental diabetic retinopathy in rats. Br J Ophthalmol 2008;92:545–547
20. Kielczewski JL, Li Calzi S, Shaw LC, et al. Free insulin-like growth factor binding protein-3 (IGFBP-3) reduces retinal vascular permeability in association with a reduction of acid sphingomyelinase (ASMase). Invest Ophthalmol Vis Sci 2011;52:8278–8286
21. Bhatwadekar AD, Guerin EP, Jarajapu YP, et al. Transient inhibition of transforming growth factor-beta1 in human diabetic CD34+ cells enhances vascular reparative functions. Diabetes 2010;59:2010–2019
22. Van Geest RJ, Klaassen I, Vogels IM, Van Noorden CJ, Schlingemann RO. Differential TGF-beta signaling in retinal vascular cells: a role in diabetic retinopathy? Invest Ophthalmol Vis Sci 2010;51:1857–1865
23. Young ME, Wilson CR, Razeghi P, Guthrie PH, Taegtmeyer H. Alterations of the circadian clock in the heart by streptozotocin-induced diabetes. J Mol Cell Cardiol 2002;34:223–231
24. Marcheva B, Ramsey KM, Buhr ED, et al. Disruption of the clock components CLOCK and BMAL1 leads to hypoinsulinaemia and diabetes. Nature 2010;466:627–631
25. Dallmann R, Touma C, Palme R, Albrecht U, Steinlechner S. Impaired daily glucocorticoid rhythm in Per1 (Brd) mice. J Comp Physiol A Neuroethol Sens Neural Behav Physiol 2006;192:769–775
26. So AY, Bernal TU, Pillsbury ML, Yamamoto KR, Feldman BJ. Glucocorticoid regulation of the circadian clock modulates glucose homeostasis. Proc Natl Acad Sci U S A 2009;106:17582–17587
27. Nagareddy PR, Xia Z, McNeill JH, MacLeod KM. Increased expression of iNOS is associated with endothelial dysfunction and impaired pressor responsiveness in streptozotocin-induced diabetes. Am J Physiol Heart Circ Physiol 2005;289:H2144–H2152
28. Abu El-Asrar AM, Desmet S, Meersschaert A, Dralands L, Missotten L, Geboes K. Expression of the inducible isoform of nitric oxide synthase in the retinas of human subjects with diabetes mellitus. Am J Ophthalmol 2001;132:551–556
29. Du Y, Smith MA, Miller CM, Kern TS. Diabetes-induced nitrative stress in the retina, and correction by aminoguanidine. J Neurochem 2002;80:771–779
30. Li Q, Verma A, Han PY, et al. Diabetic eNOS-knockout mice develop accelerated retinopathy. Invest Ophthalmol Vis Sci 2010;51:5240–5246
31. Ju WK, Neufeld AH. Cellular localization of cyclooxygenase-1 and cyclooxygenase-2 in the normal mouse, rat, and human retina. J Comp Neurol 2002;452:392–399
32. Yanni SE, McCollum GW, Penn JS. Genetic deletion of COX-2 diminishes VEGF production in mouse retinal Müller cells. Exp Eye Res 2010;91:34–41
33. Ayalasomayajula SP, Kompella UB. Celecoxib, a selective cyclooxygenase-2 inhibitor, inhibits retinal vascular endothelial growth factor expression and vascular leakage in a streptozotocin-induced diabetic rat model. Eur J Pharmacol 2003;458:283–289
34. Kuiper EJ, van Zijderveld R, Roestenberg P, et al. Connective tissue growth factor is necessary for retinal capillary basal lamina thickening in diabetic mice. J Histochem Cytochem 2008;56:785–792
35. Wood PA, Yang X, Taber A, et al. Period 2 mutation accelerates ApcMin/+ tumorigenesis. Mol Cancer Res 2008;6:1786–1793
36. Zhang B, Zhou KK, Ma JX. Inhibition of connective tissue growth factor overexpression in diabetic retinopathy by SERPINA3K via blocking the WNT/beta-catenin pathway. Diabetes 2010;59:1809–1816
37. Tikellis C, Cooper ME, Twigg SM, Burns WC, Tolcos M. Connective tissue growth factor is up-regulated in the diabetic retina: amelioration by angiotensin-converting enzyme inhibition. Endocrinology 2004;145:860–866
38. Kuiper EJ, Witmer AN, Klaassen I, Oliver N, Goldschmeding R, Schlingemann RO. Differential expression of connective tissue growth factor in microglia and pericytes in the human diabetic retina. Br J Ophthalmol 2004;88:1082–1087
39. Neves D, Santos J, Tomada N, Almeida H, Vendeira P. Aging and orchidectomy modulate expression of VEGF receptors (Flt-1 and Flk-1) on corpus cavernosum of the rat. Ann NY Acad Sci 2006;1067:164–172
40. Rahimi N. VEGFR-1 and VEGFR-2: two non-identical twins with a unique physiognomy. Front Biosci 2006;11:818–829
41. Murata T, Nakagawa K, Khalil A, Ishibashi T, Inomata H, Sueishi K. The relation between expression of vascular endothelial growth factor and breakdown of the blood-retinal barrier in diabetic rat retinas. Lab Invest 1996;74:819–825
42. Orlandi A, Chavakis E, Seeger F, Tjwa M, Zeiher AM, Dimmeler S. Long-term diabetes impairs repopulation of hematopoietic progenitor cells and dysregulates the cytokine expression in the bone marrow microenvironment in mice. Basic Res Cardiol 2010;105:703–712
43. Hazra S, Jarajapu YP, Stepps V, Caballero S, et al. Effect of Long-Term Type 1 Diabetes on Hematopoietic Stem Cells: Implications for Reduced Vascular Repair and Development of Diabetic Microvascular Complications. Diabetologia. In press
44. Wang CY, Wen MS, Wang HW, et al. Increased vascular senescence and impaired endothelial progenitor cell function mediated by mutation of circadian gene Per2. Circulation 2008;118:2166–2173
45. Zhang X, Tang N, Hadden TJ, Rishi AK. Akt, FoxO and regulation of apoptosis. Biochim Biophys Acta 2011;1813:1978–1986
46. Tothova Z, Kollipara R, Huntly BJ, et al. FoxOs are critical mediators of hematopoietic stem cell resistance to physiologic oxidative stress. Cell 2007;128:325–339
47. Artico M, Bosco S, Cavallotti C, et al. Noradrenergic and cholinergic innervation of the bone marrow. Int J Mol Med 2002;10:77–80
48. Maxfield EK, Cameron NE, Cotter MA. Effects of diabetes on reactivity of sciatic vasa nervorum in rats. J Diabetes Complications 1997;11:47–55
49. Jeong JO, Kim MO, Kim H, et al. Dual angiogenic and neurotrophic effects of bone marrow-derived endothelial progenitor cells on diabetic neuropathy. Circulation 2009;119:699–708